EPA United States Environmental Protection Agency

Monitoring of a Controlled DNAPL Spill Using a Prototype Dielectric Logging Tool

RESEARCH AND DEVELOPMENT

EPA/600/R-06/092
September 2006
www.epa.gov

Monitoring of a Controlled DNAPL Spill Using a Prototype Dielectric Logging Tool

by

Philip J. Brown II[1]
Aldo T. Mazzella[2]
David L. Wright[1]

[1]U.S. Department of the Interior
U.S. Geological Survey
Denver, CO 80225

[2]U.S. Environmental Protection Agency
Office of Research and Development
National Exposure Research Laboratory
Environmental Sciences Division
Las Vegas, NV 89119

U.S. Environmental Protection Agency
Office of Research and Development
Washington, DC 20460

267cmb06

Notice

This research was supported by the United States Geological Survey, Mineral Resources Program, and the U.S. Environmental Protection Agency under Interagency Agreement DW14937586-01-0. It has been subjected to the Agency's peer and administrative review and has been approved for publication as an EPA document. Mention of trade names or commercial products is for identification purposes only and does not constitute endorsement or recommendation by the U.S. EPA or USGS for use.

Acknowledgements

We acknowledge the Lawrence Berkeley National Laboratory and the University of California at Berkeley for providing the research facility at the Richmond Field Station. A special thanks to Dr. Karl Ellefsen of the USGS for his assistance with the FDTD modeling, to Dr. Robert Horton of the USGS for providing the preliminary petrophysical laboratory results, and to John Zimmerman of the U.S. EPA for the gas chromatograph (GC) tetrachloroethylene (PCE) analysis of the excavated tank samples.

Table of Contents

List of Figures

List of Tables

Abstract

The U.S. Geological Survey (USGS) utilized its prototype dielectric logging tool to monitor a controlled Dense Non-Aqueous Phase Liquid (DNAPL) spill into a large tank located at the University of California Richmond Field Station (RFS) containing multiple sand and clayey sand layers. To assist in the interpretation of the logging results, finite-difference time-domain (FDTD) numerical simulations were performed using a model that approximated the physical experiment. Modeling results agree well with the physical results and demonstrate qualitatively how the tool responded to the DNAPL spilled in the tank. Logging results show that the tool successfully monitored DNAPL movement throughout the duration of the experiment and was sensitive to changes in relative DNAPL saturation. Anomalous zones in the data correspond to areas where DNAPL was observed in images recorded by a color borehole video camera. Results presented in this discussion suggest that a quantitative interpretation of the dielectric tool data is possible given necessary system calibration data.

Introduction

The dielectric permittivity of a material is a measure of a material's ability to store charge when an electric field is applied (Sheriff, 1991). Often this property is denoted relative to the dielectric permittivity of free-space, resulting in a dimensionless quantity known as the relative dielectric permittivity, ε_r. In the petroleum industry, dielectric permittivity measurements can be used to distinguish between water and oil saturated zones because of the large contrast between the relative dielectric permittivity of the two zones. The relative dielectric permittivity is approximately 80 for water and approximately 2 for oil. When these fluids are present in the pore space of a typical sand reservoir, a factor of about 8 may be observed between the relative dielectric permittivity of the water versus oil saturated zones. If assumptions are made on the dielectric mixing of the components (water, oil, and sand), models can be used to determine the amount of oil in a formation (Wright and Nelson, 1993; Abraham, 1999a, 1999b).

Non-Aqueous Phase Liquids (NAPLs) comprise one of the largest classes of ground-water contaminants in the country (Lucius et al., 1992). The irregular and unpredictable migration patterns of the chemicals make mapping and monitoring the extent of contamination difficult without point measurements (Sneddon et al., 2000). Previous studies have shown that dielectric measurements can detect and monitor Light Non-Aqueous Phase Liquids (LNPLs) such as gasoline and Dense Non-Aqueous Phase Liquids (DNAPLs) such as tetrachloroethylene (PCE) (Wright et al., 1993; Wright et al., 1998; Greenhouse et al., 1993; Abraham, 1999a, 1999b; Sneddon et al., 2000; and Ellefsen, 2004). Previous controlled spill experiments have shown that surface and cross-borehole ground penetrating radar (GPR) surveys can also detect subsurface NAPLs (Greenhouse et al., 1993). The velocity of the radar wave has a strong dependency upon the dielectric permittivity (Sears et al., 1987). An independent measurement of dielectric permittivity can provide a better interpretation of GPR data.

Typical oil field dielectric logging tools are much larger than 5 cm (2-in), have a vertical resolution of about 20 cm (8-in), and are usually operated at a single frequency. This prevents their use for investigations in the shallow, small diameter wells used for environmental monitoring. For this reason, the USGS developed a prototype dielectric logging tool for application to environmental problems. The USGS tool is different from its oil field counterparts in several ways. The USGS prototype dielectric tool has a 4.45-cm (1.75-in) outer diameter (OD) allowing it to be deployed in the 5.08-cm (2-in) slim-holes often used for ground-water sampling and monitoring. It has a simple modular design allowing for easy decontamination. Most importantly, it is a time-domain tool that records data containing broad frequency content. Theoretically, the broad frequency content allows for the study of frequency dependent dielectric permittivity. Prior to this study, the USGS tool has been characterized in the laboratory (Wright and Nelson, 1993; Abraham 1999a, 1999b) and field-tested at the South Carolina Savannah River Site (Wright et al., 1998). The purpose of the current research is to evaluate the detection limits and effectiveness of the tool for monitoring DNAPL migration in the subsurface.

In May 2004, a controlled spill of the DNAPL PCE was conducted in a water-saturated tank containing multiple sand and clayey sand layers at the University of California Richmond Field Station (RFS). The experimental goal was to evaluate the detection limits of various surface and downhole geophysical techniques for monitoring the movement and location of the PCE during the controlled spill. This would allow a direct comparison of the sensitivity of the different methods and subsequent possible joint inversion (data fusion) of multiple methods for better interpretations. Techniques evaluated included surface ground penetrating radar, cross-borehole radar, directional-borehole radar, cross-borehole high frequency seismic measurements, borehole and cross-borehole complex resistivity (CR), borehole self-potential (SP), surface high-frequency frequency-domain electromagnetic soundings, surface very-early-

time time-domain electromagnetic measurements, borehole video, and dielectric logging. This discussion focuses on the dielectric logging results.

The Dielectric Logging Tool

The dielectric logging tool consists of eight main components (Figure 1). These are a fiberglass, brass-capped sonde containing the transmitter (Tx) and receiver (Rx), a sheathed 36.58 m (120 ft) long bundle of three low-loss coaxial cables, a draw-works containing the transmitter pulser, a draw-works motor controller, an optical encoder mounted to a sheave wheel, a Tektronix TDS 820 two channel digitizing oscilloscope, and a personal computer (PC).

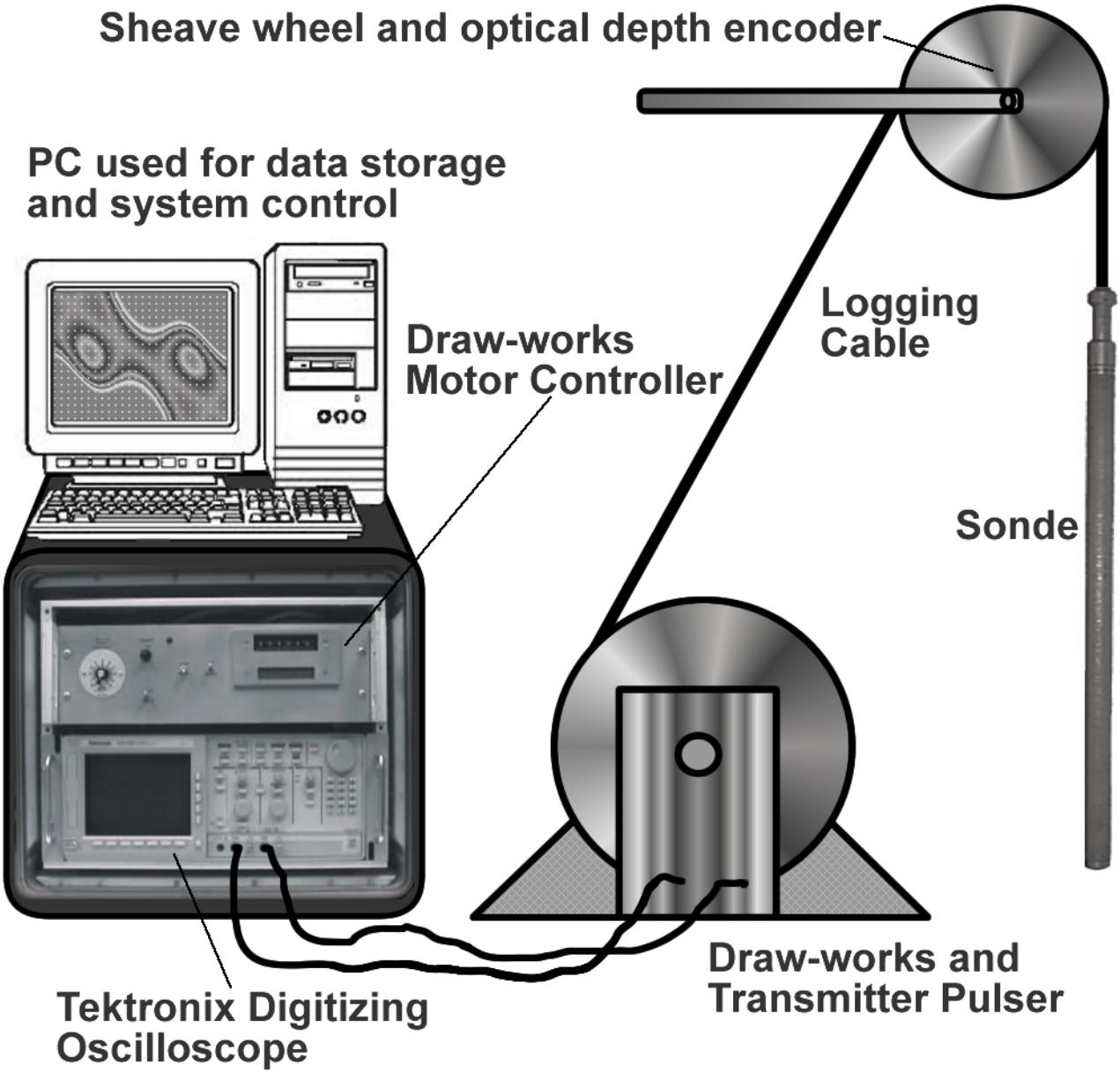

Figure 1. Illustration of the USGS prototype slim-hole time-domain dielectric logging system, not to scale.

Figure 2 shows images and a cross section of the dielectric tool. The dielectric tool's transmitter and receiver are circular plate voltage gaps that act as radial waveguides. The Tx is designed to transmit a short duration pulse, about 6 nanoseconds (ns) wide, with a very fast nanosecond rise-time into the medium surrounding the tool. A pulsed time-domain design was chosen rather than a frequency-domain design in order to rapidly obtain broad-spectrum data. A voltage gap Tx was chosen because it is difficult to drive a current loop at high frequencies since the impedance of a current loop increases with increasing frequency (Kraus, 1950).

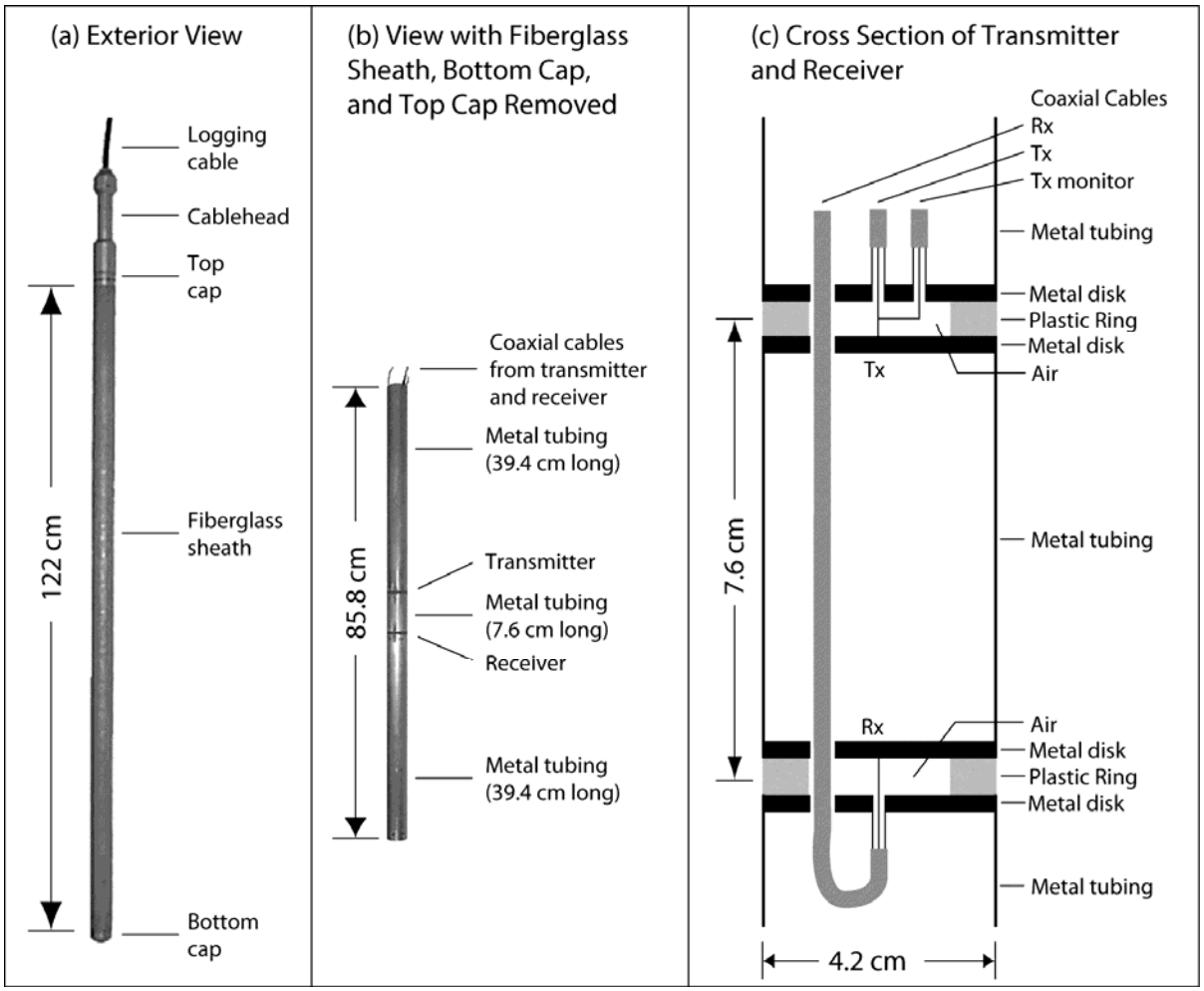

Figure 2. Prototype dielectric logging tool. Panels (b) and (c) show the 7.6-cm spacing between the Tx and the Rx as it was configured for the RFS experiment. Other tool configurations replace the metal tubing resulting in 14.6-cm or 29.9-cm Tx and Rx spacings (from Ellefsen et al., 2004).

Both the Tx and Rx consist of two metal disks and a plastic ring used to keep the disks apart and parallel to each other. Attached to each of these disks is a coaxial cable, one used to drive the Tx and another to receive the signal from the Rx. The Tx also has an additional attached coaxial cable that is used to monitor the transmitter driving voltage. All three coaxial cables have a characteristic impedance of 50 ohms. Between the Tx and the Rx is a metal tube that can be one of three different lengths. This allows

for a transmitter and receiver spacing of 7.6, 14.6, or 29.9 cm (measured from the midpoints of the Tx and Rx). The RFS spill experiment was logged with the tool using the 7.6-cm Tx to Rx spacing. For a more comprehensive discussion of the dielectric tool design, refer to Abraham, 1999a.

During data collection, a voltage pulse is generated by the electronics contained within the system's draw-works at the ground surface. This pulse is transmitted via a coaxial cable contained within the sheathed logging cable and then along the coaxial cable contained within the sonde of the tool. When the pulse reaches the transmitter, it is radiated from the voltage gap. This pulse then propagates along the tool as well as into the borehole and strata radially out from the borehole. The direct radiated field and reflections are picked up at the Rx producing a voltage pulse that is transmitted to the surface via the Rx coaxial cable in the tool and the logging cable. At the surface, the analog signal is digitized by the 16 bit Tektronix TDS 820 oscilloscope and recorded by a PC. Recording of the received signal starts approximately 1.5-ns before Tx turn-on and lasts until approximately 21.5 ns after Tx turn-off. Each trace consists of 2,500 samples with a sample interval of 0.01 ns, giving a trace duration of 25 ns. For a more complete discussion of the wave propagation modes set up by the dielectric logging tool, refer to Ellefsen et al., 2004.

The Physical Experiment

The current experiment was conducted in a nonmetallic, fiberglass tank that was housed in a special building at the University of California Richmond Field Station that had been designed to minimize electromagnetic coupling and electrical noise interference for geophysical research. The tank is about 2.4 meters in diameter and 1.8 meters in depth and was constructed with PCE-resistant resin (Figure 3). Two other barriers were in place outside the tank to prevent any PCE leakage to the outside environment. A multilayer formation consisting of sand and clayey-sand layers was engineered and constructed in the tank. It was necessary to consider various factors in the construction of the formation. These included a balance between the presence of clay needed for the induced polarization response for the CR method and high formation resistivity needed for the GPR method. In addition, the layers had to have good hydraulic conductivity to allow the PCE to penetrate into the formation within a reasonable time period of a few days and the ability to effectively allow the removal of air in the formation pore space for good seismic signals. The final configuration was developed after a number of experimental laboratory studies were conducted.

The layers in the tank were constructed with a washed, well-sorted medium grain sand, Unimin 20/30. This is composed of over 99% SO_2. Laboratory measurements showed that the packed sand had a porosity of about 36%. A number of time-domain reflectometer (TDR) measurements indicated a range in porosity from 35 to 39% at different locations about 7 cm apart in a water saturated packed sand cylinder. A calcium montmorillonite clay, SAz-1, obtained from the National Clay Repository at Purdue University was used for the development of the clay/sand layers. The central portion of the tank, with a diameter of about 1 meter, was the primary area for the experiment. The formation in this area consisted of three layers, a 53-cm thick upper sand layer, a 20-cm thick 3% clay/sand layer overlying a 30-cm thick 6% clay/sand layer (dry weights). Beneath this, a 3-cm thick solid clay barrier was placed to prevent the PCE from migrating directly to the bottom of the tank. Below the solid clay barrier, a sand layer about 47 cm thick extended to the bottom of the tank. The horizontal extent of these layers was confined with a thin vertical plexiglass sheet that formed a cylinder around the volume that was about 70 cm high and 100 cm in diameter. The sheet was embedded about 1 cm into the solid clay barrier. The formations were fully saturated during construction with a 0.001 M calcium chloride distilled water solution. The conductivity of the water was about 230 microseimens/cm. Preliminary results of a petrophysical analysis of the materials in the tank can be found in Table 1. A number of clear polyvinyl chloride (PVC) and clear acrylic closed wells and probes were placed in the formation during construction to accommodate the different geophysical methods (Figure 3). The east and west cased wells ran from approximately 12 cm above the sand to the bottom of the tank and had an inner diameter (ID) of 7.62 cm (3 in). The north and south observation wells ran from about 27 cm above the sand and had an ID of 5.08 cm (2 in). The two larger ID east and west wells were continuously logged with geophysical instruments and all of the wells were logged using borehole video equipment. The dielectric logging presented in this paper was conducted in the west well.

After construction, the formation was monitored and allowed to stabilize for about two months. About 10 days before the injection experiment began, monitoring with the complex resistivity and seismic measurements established the formation stability. About five days before the injection began, monitoring with all the geophysical methods established pre-spill background baselines and noise levels.

In May 2004, the injection experiment began. Eighty-five (85) liters of PCE was injected over a period of 26 hours into the subsurface at a fairly constant rate of about 3.7 liters/hour. In order to track the migration of the PCE with downhole video and subsequent excavation, a dye, Oil Red O, was added to

(a)

(b)

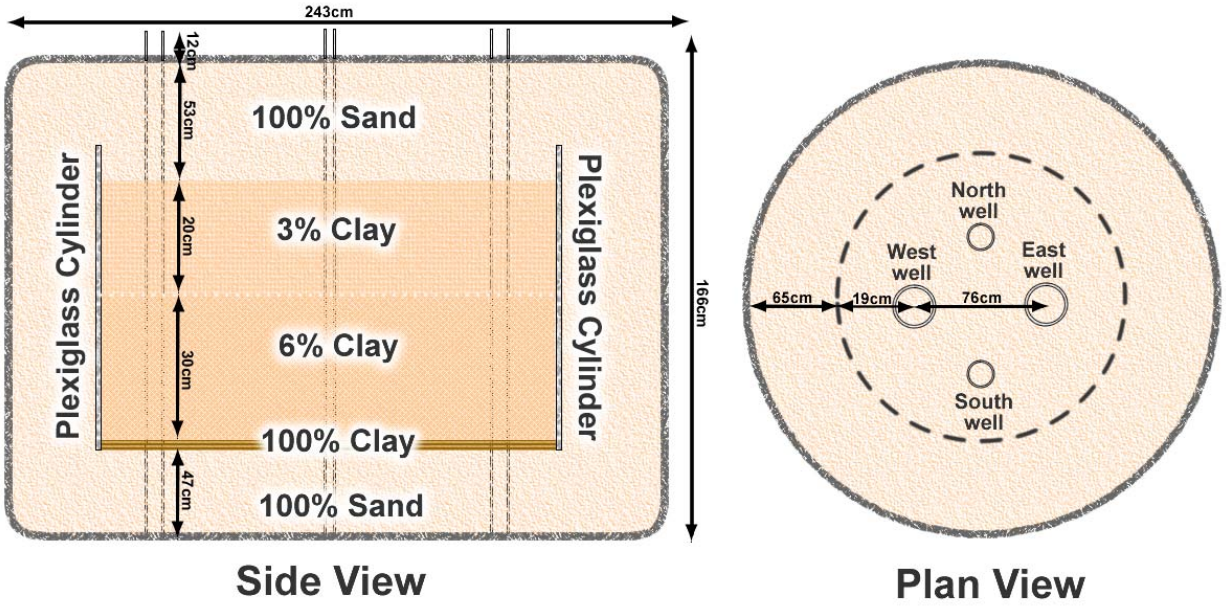

(c)

Figure 3. (a) Photograph of the fiberglass tank cylinder used for the controlled PCE spill experiment. The tank was located inside two other barriers to prevent any PCE leakage to the outside environment. (b) Photograph of the completed sand and clay/sand formations in the tank. North is to the right in the photograph. The west well is at the top of the photograph. (c) Schematic of the fiberglass tank is not to scale. The dielectric logging presented in this report was in the west well. For clarity, the location of other downhole CR probes and seismic wells positioned near the north and south wells are not shown in the schematic.

the PCE at a concentration of 3.0 g/L. The PCE was injected through a tube in the center of the tank at a depth of about 6 cm below the surface. The injection tube extended 24 cm above the surface. This allowed a sufficient head to develop to overcome surface tension effects and the PCE flowed into formation. A plot of the PCE injected volume as a function of time is shown in Figure 4. Before the injection began, the water table had been established at about 1 cm above the surface of the sand. In order to maintain a constant fluid level in the tank, the water displaced by the PCE during injection was

SAMPLE	Two-electrode resistivity (ohm-m)	Two-electrode resistivity (ohm-m)	ε_r	PCE residual percentage of pore volume
	10 0Hz	10 MHz	10 MHz	%
Unimin sand	178	178	23.9	16.4
3% clay	75.8	46.7	23.4	13.3
6% clay	61.1	3 4.2	31.4	10.6
ABC	–	–	7.56	–

Table 1. Preliminary petrophysical analysis of the materials in the sand tank is shown in Table 1. The Unimin sand is 100% water saturated with 1.0 mM $CaCl_2$ solution. The 3% clay is 3% SAz-1 clay (dry wt.) mixed with Unimin sand, saturated with 1.0 mM $CaCl_2$ solution. The high dielectric value (31.6) for the 6% clay is not fully understood. Time-domain reflectometry measurements during construction of the formation layers indicated dielectric values of about 24 for the 6% clay. The difference may be due to the different frequency spectra of the two measurements. The ABC clay is the same 100% block clay used in the experiment as received. The PCE residual is the percent of the pore volume retained in the sample after flushing with 1.0 mM $CaCl_2$ with a 5-cm head. A 36% porosity value was used for the samples. These PCE residual values are comparable to the dielectric tool BHS analysis and the GC results of the samples from the tank excavation.

siphoned off to an external reservoir. Because of the limited space and interference effects between different systems, a schedule was established when data with the different geophysical methods would be obtained.

Pre-spill data were obtained with the borehole dielectric tool at 104, 57, 5, and 4 hours before the injection began. Post spill data were collected about 4, 15, 59, 79, 90, 112, 137, and 158 hours after the injection started. The first two measurements (at 4 and 15 hours) were obtained during the injection period and the last six were after the injection stopped. These were the start times for the logging; it took about 30 minutes to acquire a data set.

Data Collection Procedure

All dielectric logging was performed in the west well of the tank (Figure 3c). For all tests, the experimental setup remained the same with all electronics and required support equipment in the same position relative to the tool. Logging speed was maintained by the computer-interfaced electronic draw-works and held constant at approximately 1 mm per second. Zero depth was set for the optical encoder when the Rx was at the same level as the top of casing. The tool was run to the bottom of the hole and stopped. The depth level was then checked to ensure it was consistent with other logging runs. For any one logging run, the tool was never more than 5 mm off in depth from any other logging run. Data were recorded while the tool was being pulled out of the hole and the computer automatically stopped the system when the tool reached zero depth. The logging sonde was kept in the middle of the hole by polystyrene centralizers affixed to the head, tail, and midpoint of the tool. All data were collected with the tool running in continuous data acquisition mode as opposed to a start and stop mode. To reduce radio interference in the received signal from various sources at the site, each final record is an average of two repeat logging runs of four-stack data.

Before the spill began, four background measurements were logged in the tank over a 2-day period. Each final background measurement was the average of two logging runs of four-stack data with the exception of the first background measurement that was only two-stack data. This was done to get a base level to compare to the monitoring measurements made during and after the spill as well as to demonstrate the

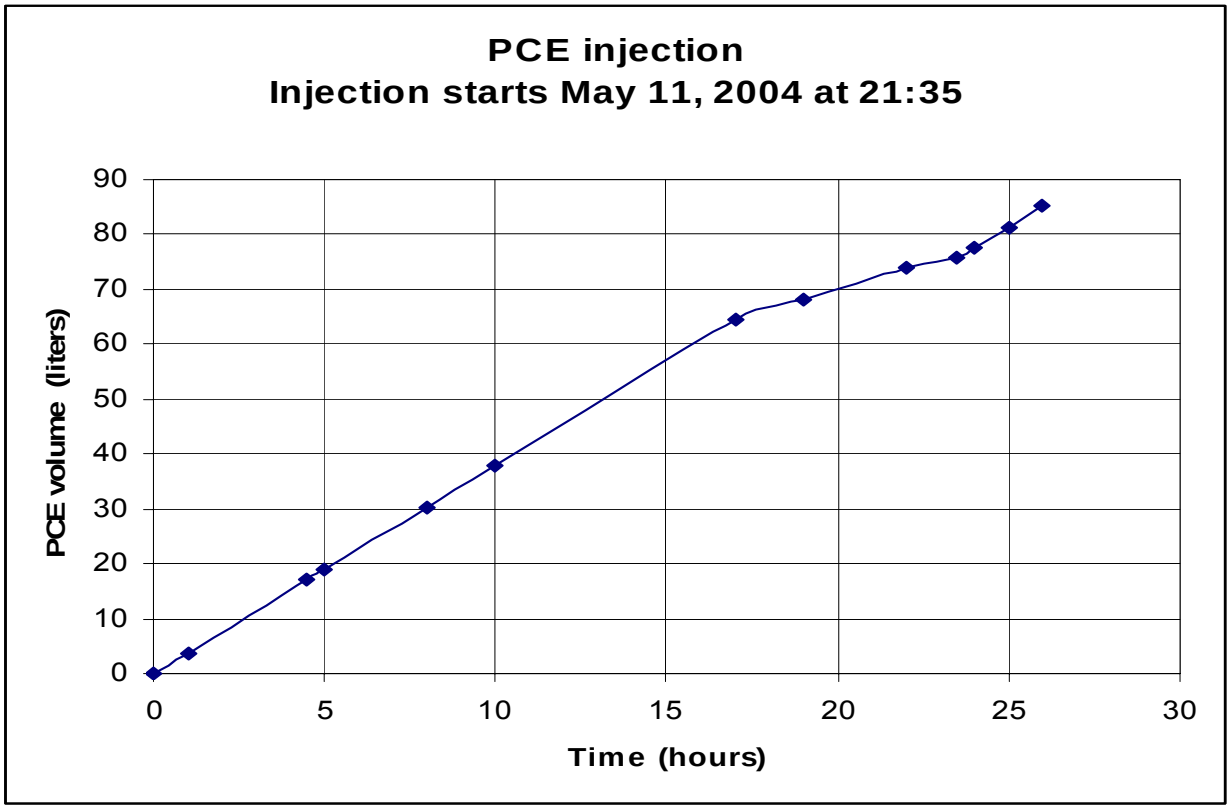

Figure 4. Plot of PCE injection volume verses time for the May 11, 2004 controlled spill experiment.

reproducibility of the dielectric tool data. These data are plotted in Figures 5 and 6. The depths indicated are from the top of the well casing which was about 12 cm above the surface of the sand. The data in Figure 5 are shown as color amplitude plots for the recorded trace time at each depth for each of the four background measurements. An average of these four data sets was used as the pre-spill background baseline and is shown on the right of Figure 5. The data plotted in Figure 6 are the voltage amplitude verses recorded trace time for each of the four background measurements at a depth of 65 cm (53 cm below the surface); this is at the top of the 3% clay/sand layer. Note the noise shown in the oldest background measurement (Figure 5 and 6; 105 hours pre-spill); this is believed to come from a local AM radio transmission tower located about 1 mile from the site. This noise is larger on this first data set because only two stacks were acquired. All subsequent data represent four stacks resulting in the noise being considerably reduced. A maximum variation of 3.7% is observed in the peak amplitude among the four different background measurements acquired over the 2-day pre-spill period.

Data Reduction

Once data are recorded, very little data processing is required. The time base for the system is stable so that no traces need to be adjusted temporally to account for late or early triggering of the Tx or Rx. From trace to trace, there is a small static offset in the record before turn-on. To correct for this offset, the average voltage for the first 70 samples of the record are subtracted from the entire record normalizing the pre turn-on part of the trace to approximately zero volts. After the traces have been static shifted, correction factors are applied to account for attenuators that exist at the draw-works. No correction is made for the attenuation of the received signal through the 36.58 m of logging cable. Data from four

repeat logging runs were then averaged to further reduce the radio noise that was seen in the data. After the data were averaged, the data were gridded using the minimum curvature method and a grid cell size of 2 mm. Once the data were gridded, the average background data were subtracted from the data recorded after the PCE injection began. This produces residual data where changes occurring due to the PCE are more apparent.

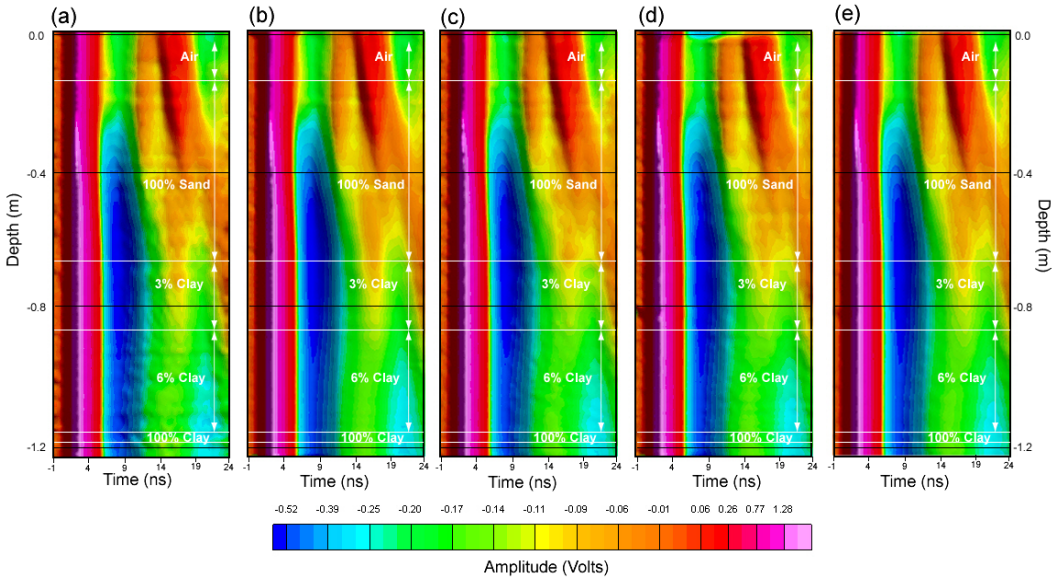

Figure 5. Pre-spill background dielectric logging measurements taken at (a) 104, (b) 57, (c) 5, and (d) 4 hours before the injection started. Plot (e) is the average of plots (a), (b), (c), and (d). The color scale represents the recorded voltage, the vertical scale is the logging depth below the top of the borehole, and the horizontal scale is the recorded trace time. Note the additional radio noise in plot (a). This is due to these data only having two stacks per record instead of four stacks.

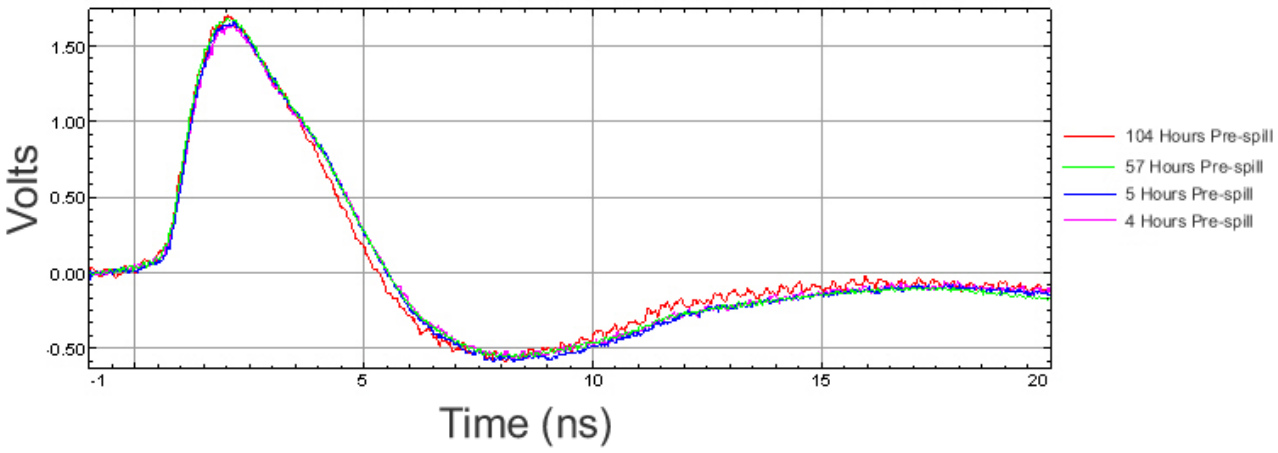

Figure 6. Dielectric waveforms at 65-cm depth, at the top of the 3% clay layer, taken at 104, 57, 5, and 4 hours before the injection started. A maximum variation in the peak amplitude of 3.7% is observed among the four pre-spill measurements. Note the strong radio interference noise shown in the background waveform taken 104 hours before the spill. Only two stacks of the data were obtained for this first data set. Four stacks of data were acquired for subsequent data sets and the noise was considerably reduced.

Numerical Modeling

Model Description

To understand the influence of changes in DNAPL saturation on tool response, numerical simulations were performed. This modeling was accomplished using a finite-difference time-domain (FDTD) method that simulates the propagation of electromagnetic waves in time. To optimize the modeling speed, the numerical simulation takes advantage of tool and borehole symmetry by utilizing a cylindrical coordinate system where the z-axis is aligned with the borehole axis. Given this symmetry, computations only have to be performed in the r and z-directions, greatly reducing the computation time. Each model took approximately 5 hours to run on a standard PC using a 1.3-GHz AMD processor. A detailed description of the FDTD numerical simulator can be found in Ellefsen et al., 2004.

Figure 7 is a diagram of the numerical model. The physical properties used in the modeling can be found in Table 2. The upper and lower bounds used for the relative dielectric permittivity of the sand, water, and PCE mixtures are based upon research done by Sneddon et al., 2000. From Table 2 and Figure 7, it is apparent that the model is a simplification of the physical dielectric logging tool. It omits the monitoring coaxial cable found at the transmitter, the top and bottom brass caps on either end of the sonde, the cable head, and the logging cable as well as the polystyrene centralizers. Additionally, the tool is assumed to be as long as the entire borehole. Nonetheless, the FDTD model still represents important characteristics of the dielectric logging tool. It can be used to qualitatively understand the tool's early-time physical response to different borehole environments without the complications of reflections from the ends of the tool.

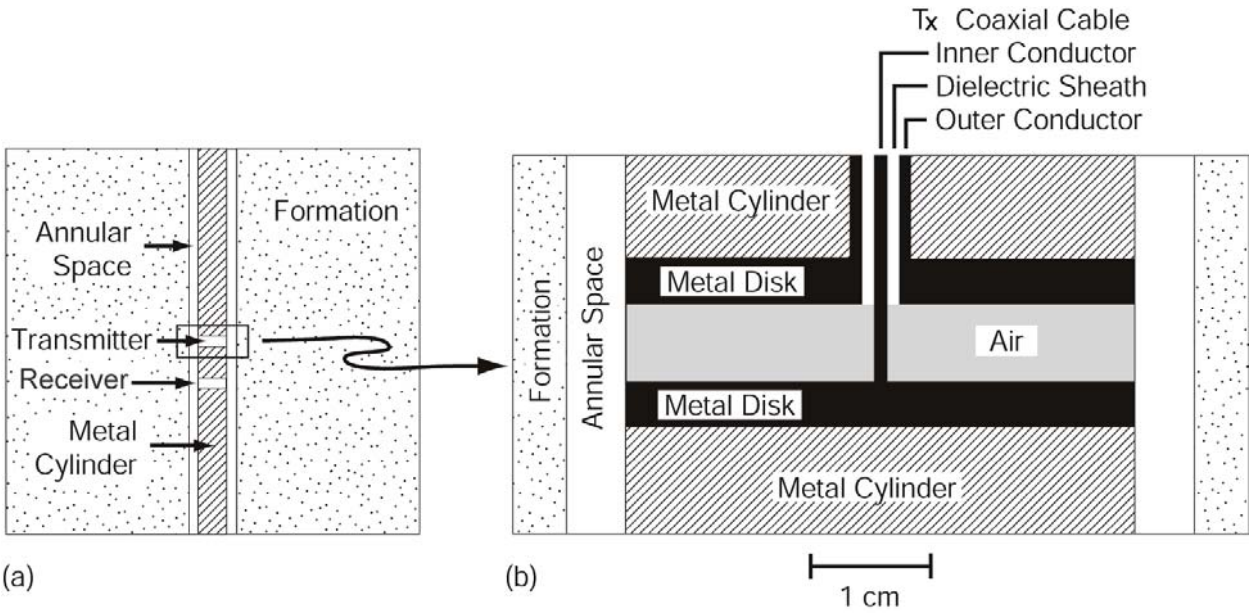

Figure 7. (a) Model used for the FDTD simulations in the numerical modeling. This diagram is not to scale. (b) Close-up of the transmitter part of the model drawn to scale. The model used for the receiver is identical to the model used for the transmitter but rotated 180 degrees. The electrical properties of the model are listed in Table 2 (after Ellefsen et al., 2004).

Table 2. Electromagnetic properties and dimensions of the model used for the FDTD simulation. Metal is represented as a perfect conductor resulting in the relative dielectric permittivity with the relative magnetic permeability having no significance.

Item	Material	Relative Dielectric Permittivity	Relative Magnetic Permeability	Electrical Conductivity (S/m)	Dimension (mm)
Inner conductor, Tx and Rx coaxial cables	Metal	---	---	∞	Outer radius: 0.5
Plastic Rings in Tx and Rx gap	Plastic	3.6	1	0	Inner radius: 12.6 Outer radius: 20.6
Outer conductor, Tx and Rx coaxial cable	Metal	---	---	∞	Inner radius: 1.5 Outer radius: 2.0
Metal cylinder above Tx and below Rx	Metal	---	---	∞	Inner radius: 2.0 Outer radius: 20.6
Metal disk above Tx and below Rx	Metal	---	---	∞	Inner radius: 2.0 Outer radius: 20.6 Axial length: 5.0
Air in Tx and Rx gap	Air	1	1	0	Inner radius: 0.5 Outer radius: 20.6 Axial length: 6.4
Metal disk below Tx and above Rx	Metal	---	---	∞	Outer radius: 20.6 Axial length: 5.0
Metal cylinder below Tx and above Rx	Metal	---	---	∞	Outer radius: 20.6
Metal cylinder	Metal	---	---	∞	Outer radius: 20.6
Annular Space	Air	1	1	0	Inner radius: 21.9 Outer radius: 38.1
Fiberglass Tool Casing	Plastic	4.5	1	0	Inner radius: 20.6 Outer radius: 21.9
Borehole Casing	Plastic	4	1	0	Inner radius: 38.1 Outer radius: 40.4
Formation	100% water saturated sand or PCE water saturated sand	24 for wet sand; 20,16, 13,10, 8, 6 and 4 for PCE and water saturated sand	1	0	Inner radius: 25.4 Outer radius: 1,500

Numerical Modeling Results

Figure 8 shows the calculated voltage response at the end of the coaxial cable connected to the receiver. The different curves represent the modeled response to formations having different relative dielectric permittivity. Figure 8 illustrates that with decreasing relative dielectric permittivity of the formation, the received voltage decreases in amplitude.

For comparison purposes, Figure 8 also displays an average of the four traces recorded in the sand portion of the RFS tank at a depth of 65 cm before the spill began. In order to match amplitudes with the physical data, the modeled data had to be scaled by a factor of 0.54. This is because the model simulates voltage at the receiver and the tool records voltage at the end of a 36.58-m cable. Such an amplitude loss in voltage over the length of the cable agrees with tests performed by Abraham, 1999a. To be consistent with the petrophysical analysis of the wet sand (Table 1), a scaling factor of 0.54 was chosen because it normalized the amplitude of the data to the modeled curve where $\varepsilon_r = 24$. A comparison of the variation in the pre-spill data (3.7% maximum variation in the peak amplitude) with the modeling results is shown in Figure 9. These results suggest that relative dielectric permittivity changes of about 4 can be determined at high dielectric values of about 20 and changes of about 1.5 can be determined at lower dielectric values of about 7.

Some characteristics of the physical data are not seen in the numerical data. The large differences are due to multiple reflections constructively and destructively interfering with each other. These reflections arrive at the receiver from the ends of the tool and the ends of the logging cable. These arrivals are not observed in the model for two reasons. The modeled tool is significantly longer than the physical tool so that these arrivals would theoretically arrive at a different time in the record and the edges of the model are absorbing boundaries that have practically no reflection, meaning that the model emulates a grid extending to infinity.

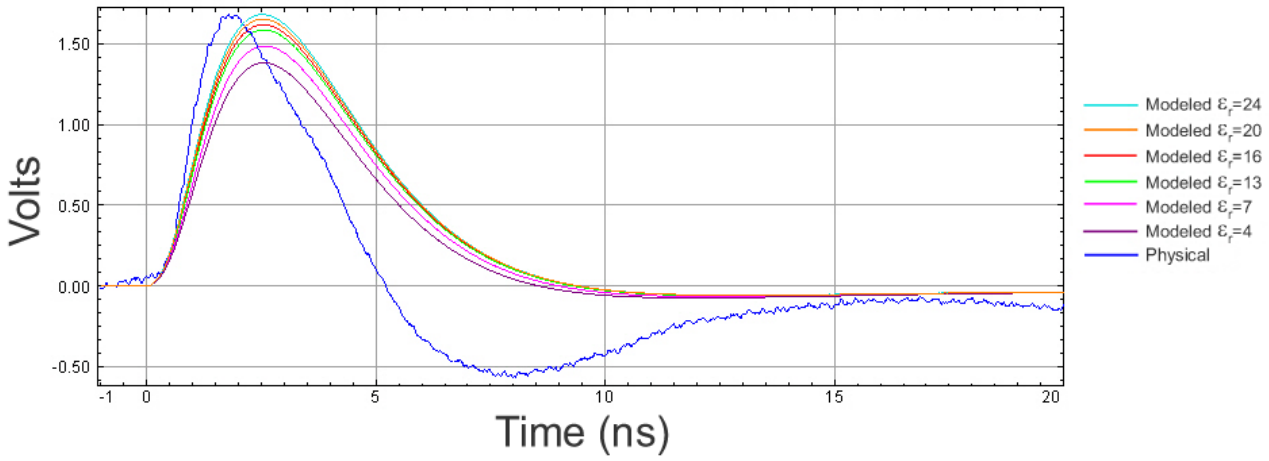

Figure 8. Plot of the modeled response for a host material around the borehole having a relative permittivity of 24, 20, 16, 13, 7, and 4. For comparison purposes, the average background physical waveform from a depth of 65 cm is plotted as well. Primary differences in the modeled and received waveform are due to multiple reflected arrivals not accounted for in the model.

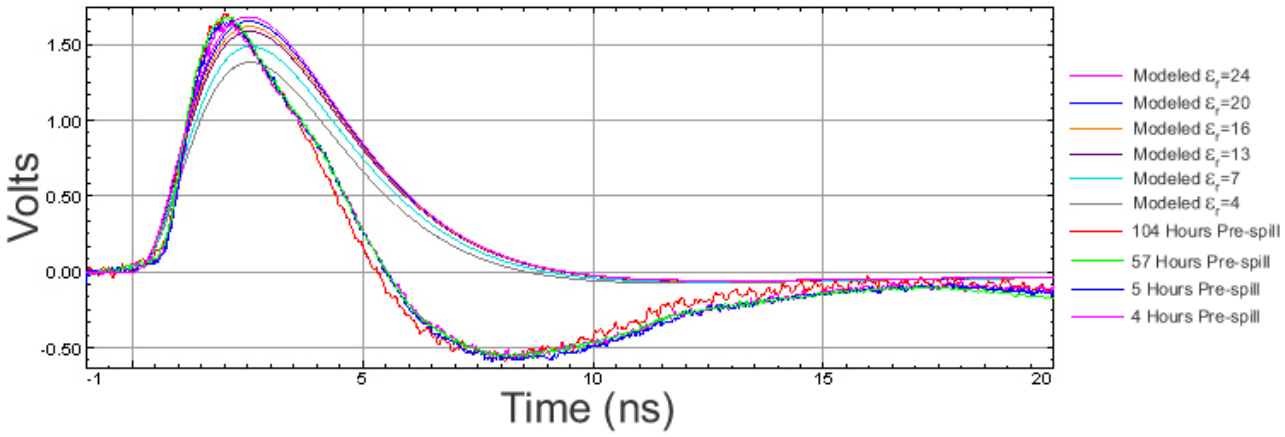

Figure 9. Plot of the four raw pre-spill (background) physical traces from a depth of 65 cm and six modeled curves. Note how radio noise is more apparent in the 104-hour pre-spill trace. This is because this trace only stacked individual waveforms two times at each data set and the others stacked individual waveforms four times. These data suggest that the dielectric logging tool can detect relative dielectric permittivity changes of about 4 at high dielectric values of about 20 and changes of about 1.5 at lower dielectric values of about 7. Based upon the BHS model, an overall uncertainty and changes in PCE saturations of about +/- 5% should be detectable given the repeatability of the system.

Physical Dielectric Logging Results and Interpretation

The average of all four background measurements can be found in Figure 10a. The horizontal white lines on this plot indicate the boundaries between various formation zones in the sand tank. Approximately four hours into the spill, two logging runs were made back to back with the dielectric tool and one run was made using a color borehole video logger. The dielectric data in Figure 10b show an anomaly that encompasses the 63-cm depth where the red-dyed PCE is first seen breaking through to the borehole wall on the video log. The plot in Figure 10c, which shows the difference between the data of Figures 10b and 10a, emphasizes this anomaly further. The thickness of the anomaly in the dielectric log is about 17 cm starting at roughly 48-cm depth and ending approximately at the contact between the 100% sand and 3% clay layers at 65-cm depth. The apparent thickness of the anomaly is probably greater than the actual thickness because of the finite Tx-Rx spacing. As predicted by the computer models, most of the traces in the anomalous zone decrease in amplitude. This is illustrated in Figure 11, which shows the modeling results compared to a trace recorded in the anomalous zone of Figures 10b and 10c. Comparing the physical and modeled data in Figures 8 and 11 suggest an average $\varepsilon_r = 7$ for the formation around the borehole. Using the Bruggerman-Hanai-Sen (BHS) mixing formula flow chart presented in Sneddon et al., 2000, this permittivity corresponds to a PCE concentration of 62% of the pore space. Based upon the uncertainty in the four pre-spill dielectric measurements (3.7%) and the BHS mixing formula, the PCE saturation can be determined with an overall uncertainty of about +/- 5% from the dielectric logging measurements.

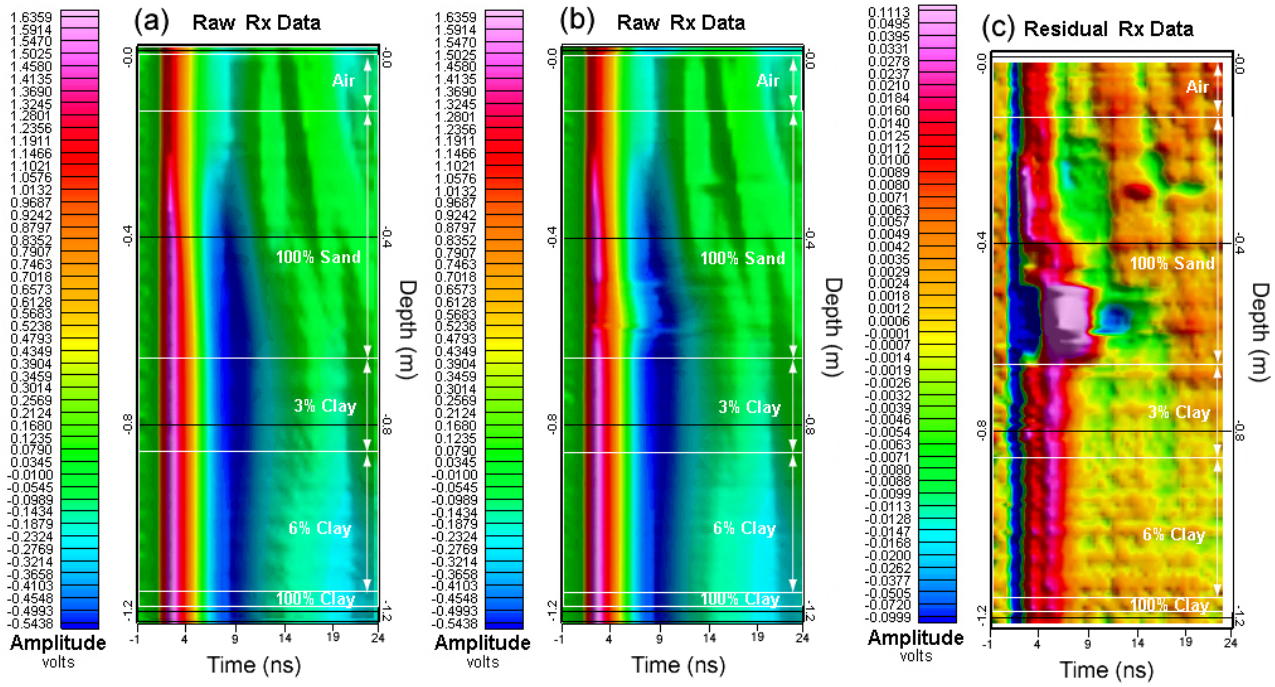

Figure 10. (a) Average raw pre-spill data, (b) average raw data four hours into the controlled PCE spill and (c) the residual of the two images. A color borehole video log taken immediately after the dielectric log shows approximately a 3-cm thick horizontal layer of DNAPL against the borehole wall at 62-cm depth (referenced to the top of the borehole). This location agrees with the bottom of the anomaly shown in the dielectric log and the top of the 3% clay layer.

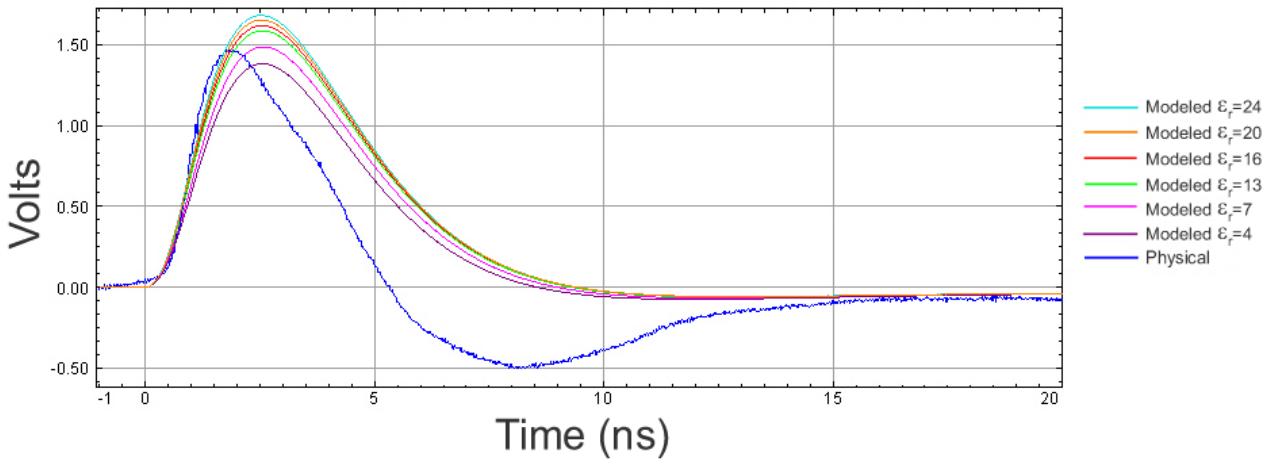

Figure 11. Plot of the modeled response for a host material around the borehole having a relative permittivity of 24, 20, 16, 13, 7, and 4. For comparison purposes, a physical waveform is plotted from the anomalous zone at 65-cm depth shown in Figure 10b and 10c. The numerical results suggest a relative dielectric permittivity of 7 for the physical data. According to the BHS flow chart found in Sneddon et al., 2000, this implies a relative PCE saturation of approximately 62%. Primary differences in the modeled and received waveform are due to multiple reflected arrivals not accounted for in the model.

Additional dielectric logs were recorded approximately 15, 59, 84, 90, 112, 137, and 158 hours after PCE injection started. The video logs confirm that the tool did track the progress of the PCE as it passed through all the layers of the tank and eventually reached the tank bottom. It can be seen that during injection, approximately four hours into the spill, the PCE is pooling on top of the 3% clay layer (Figure 10c). Approximately 15 hours into the experiment, PCE has made its way down to the 100% clay layer and the tool response to the PCE is strongest in the 6% clay layer (Figure 12a and 12b). Approximately 10 hours into the experiment, the video log showed PCE from approximately 60-cm depth to the top of the 100% clay layer (115-cm depth from the top of the well casing). This corresponds to the higher amplitude parts of the residual signal displayed in Figure 12a and Figure 12b. Figure 13 shows the data taken at 59 hours into the experiment, 33 hours after the spill stopped. A decrease is observed in the residual amplitudes between Figure 12b and Figure 13b; it appears that the PCE concentration close to the borehole in Figure 13 (at 59 hours) has decreased from the PCE concentration shown in Figure 12 taken approximately two days before.

This makes sense given that PCE was observed in the video logs below the 100% clay barrier approximately 4.5 hours into the experiment, meaning the PCE had a pathway to migrate below the 100% clay barrier during the injection period and then drain after the injection of the PCE stopped. It also agrees with the preliminary petrophysical analysis that shows that a PCE residual stays in the sand even after flushing with water (Table 1). Comparison of maximum and minimum amplitude traces recorded in the sand at depths of 31 and 60 cm in Figure 13a to the computer models suggests a relative dielectric permittivity that ranges between 24 and 20, respectively (Figure 14). According to the BHS flow chart in Sneddon et al., 2000, such a permittivity range implies a relative residual PCE saturation of between 0 and 12% of the pore space of the 100% sand. A similar analysis was conducted on the dielectric data at the 75-cm depth (middle of the 3% clay layer) and at the 100-cm depth (middle of the 6% clay layer). These results are shown in Figure 15. Based upon the peak amplitude, dielectric values of about 22 are derived. Ignoring the presence of clay for the modeling and BHS mixing-law, bulk PCE residual saturations of about 7% were derived in these layers. Based upon the four pre-spill dielectric measurements, these PCE saturation values have an uncertainty of about +/- 5%. These data confirm that

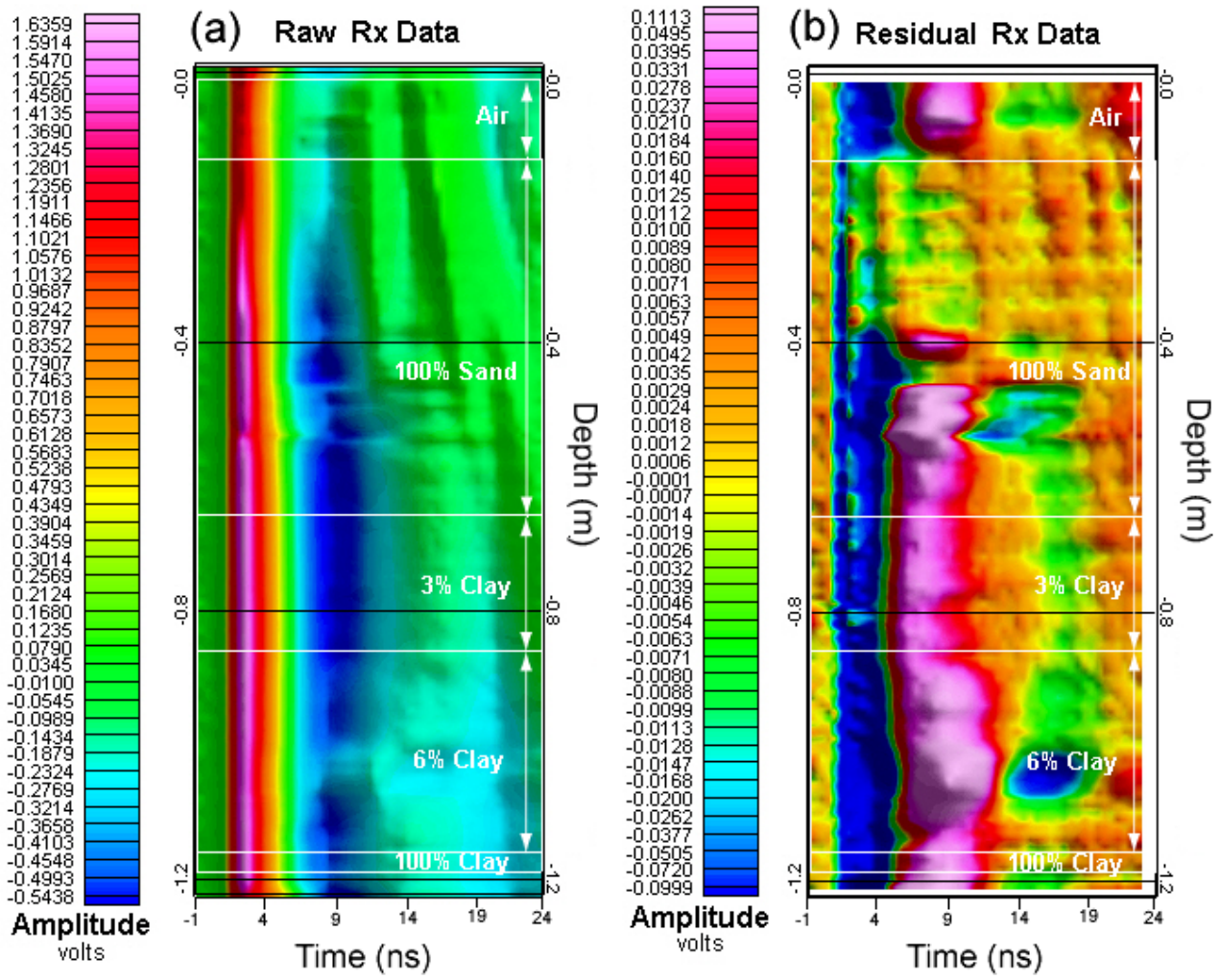

Figure 12. (a) Raw and (b) residual dielectric logging tool data collected 15 hours into the experiment during injection. The tool response appears to be strongest in the 6% clay layer.

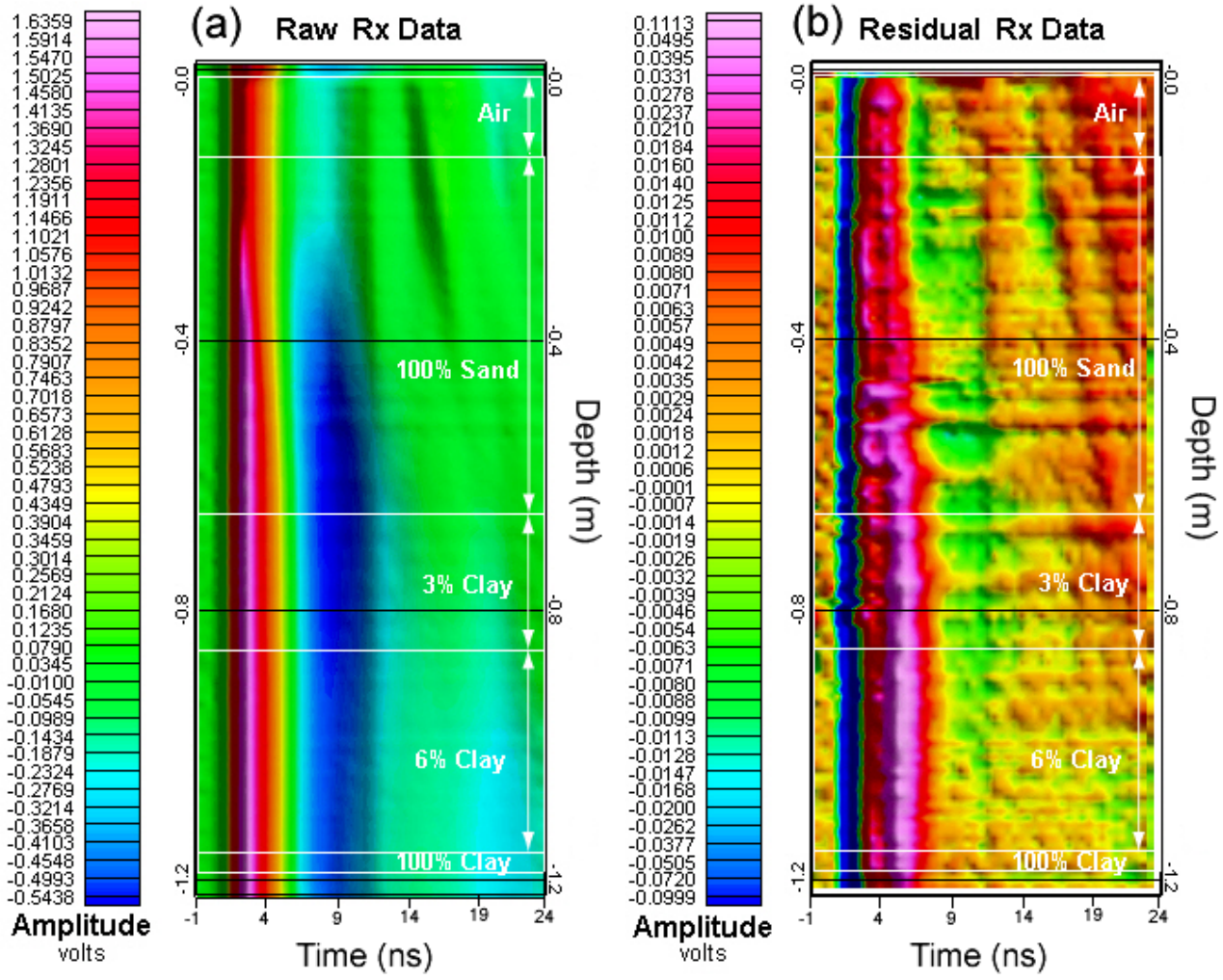

Figure 13. Raw (a) and residual data (b) collected postinjection approximately 59 hours into the experiment and approximately 33 hours after injection stopped. Note that the PCE broke through the 100% clay layer approximately four hours into the experiment. This image suggests that the PCE has flowed through the 3% and 6% clay layers and that the dielectric tool has responded to residual PCE left in the pore space. The borehole video image by this time shows PCE from approximately 60-cm depth to the top of the 100% clay layer. This correlates with the strongest part of the anomaly shown in the residual image (b).

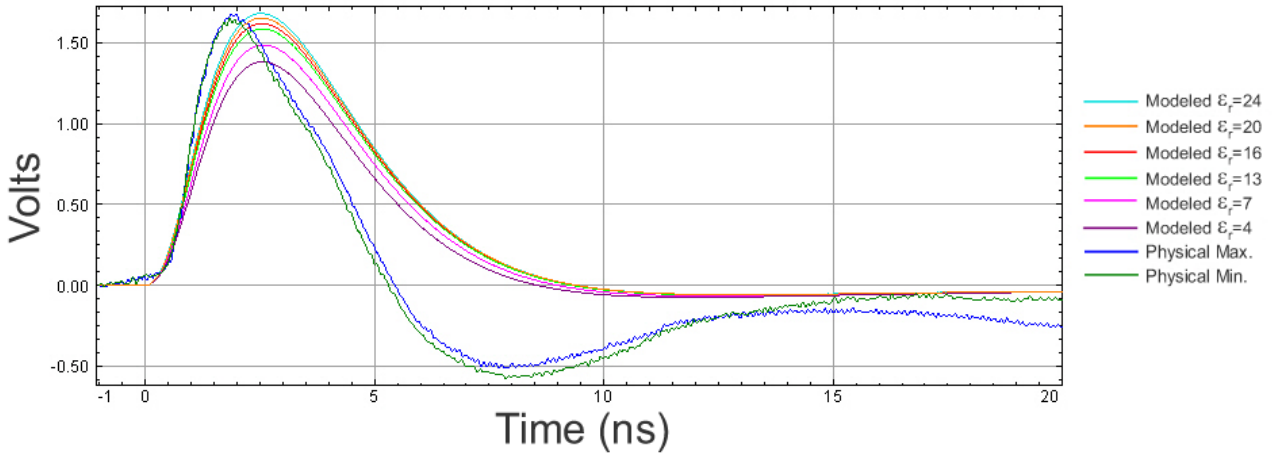

Figure 14. Example of minimum and maximum amplitude traces recorded in the 100% sand zone 33 hours after injection stopped (refer to Figure 13 at approximately 31 and 60 cm). These traces suggest a relative permittivity range in the sand between 24 and 20. According to the BHS flow chart found in Sneddon et al., 2000, this implies a relative residual saturation of PCE between 0 and 12%. These have a saturation uncertainty of about +/- 5%, based upon the pre-spill baseline measurements.

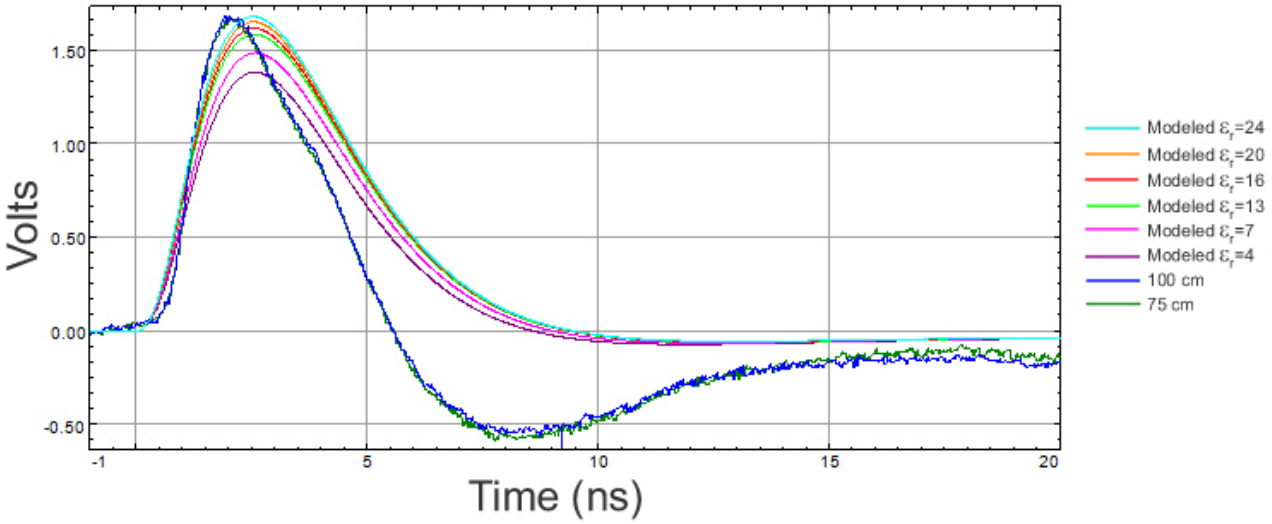

Figure 15. Amplitude traces taken at 33 hours after the injection stopped at depths of 75 cm (middle of the 3% clay layer) and at 100 cm (middle of the 6% clay layer). These traces suggest relative permittivity of about 22 and according to the BHS model implies a residual saturation of about 7%. This has a saturation uncertainty of about +/- 5%, based upon the pre-spill baseline measurements.

the dielectric logging tool can be used to monitor movement of PCE around a borehole and that the tool is sensitive to changes in the relative saturation of PCE.

Closer analysis of the data show that some traces in the anomalous PCE saturated zones have a dramatic decrease in slope approximately 1.5 ns after the peak amplitude. This is illustrated by trace 68 (62 cm) labeled in Figure 16. At first this was troublesome to the authors because such a change in slope was not seen in the modeled data. In an attempt to reproduce this response in the numerical simulation, a two-dimensional model was run that had a 100% PCE saturation at the borehole wall to a radius of 14 cm away from the borehole wall. The result of this modeling along with trace 68 for comparison can be observed in Figure 17. The modeled data agree qualitatively with the physical data. The tool may have detected at least 14 cm or more into the formation surrounding the borehole. Quantitative interpretation of the dielectric tool data is complicated by possible asymmetry and inhomogeneity of the PCE saturation surrounding the borehole.

Based upon video logging, it is estimated that by May 18, 120 hours after the spill stopped, about 72 liters of PCE had migrated to the bottom of the tank (85% of the injected volume). The remainder was retained in the layers as residual saturation. The tank was monitored by some of the other geophysical methods until March 2005. Little geophysical or video logging changes were observed during the period from the end of May 2004 until March 2005. In March 2005, the tank was drained and the formations were excavated. Based upon the Oil red O dye, significant fingering and stratification in PCE concentration were observed throughout both the 3% and 6% clay layers. Photographs of the excavated PVC wells are shown in Figure 18. Variation in the PCE distribution in the layers is evident from the distribution pattern left from the PCE etched and the Oil Red O dyed surface of the excavated PVC wells. During excavation, a number of samples of the formations were collected at about every 10-20 cm in depth. The samples were analyzed on a gas chromatograph and the results are shown in Figure 19. In the sand above 62-cm depth, the residual PCE is less than 5% of the pore space, in the 3% clay layer in ranges from 2 to 26% of the pore space, and in the 6% clay layer in ranges from 2 to 20%. Below the solid clay barrier, little residual PCE was observed, except at the very bottom of the tank (from 4 to 10%) where it had drained. Given the significant inhomogeneity of PCE concentration over short distances, these results are in reasonable agreement with the preliminary BHS analysis of the dielectric tool.

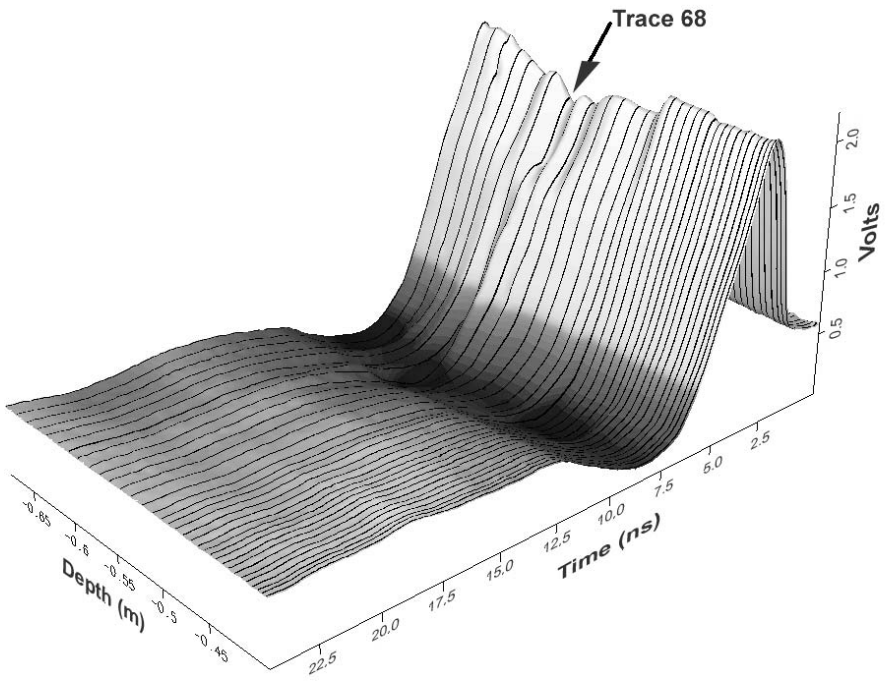

Figure 16. Magnified three-dimensional plot of the anomalous zone displayed in Figure 10b and 10c (four hours after the spill began). Note the large decrease in slope shown at trace 68 at approximately 2.5 ns. In accordance with the numerical simulation, this may be attributed to a finite vertical layer (~14 cm deep) of PCE against the borehole wall (refer to Figure 17).

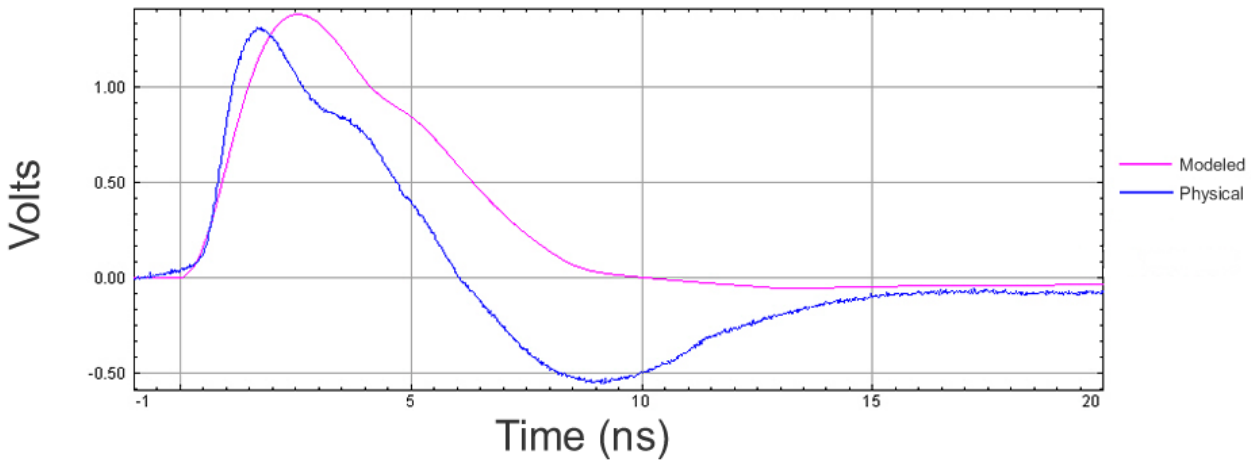

Figure 17. Plot of the raw waveform average of trace 68 (Figure 15) recorded four hours into the spill during injection at a depth of 62 cm (Figure 10b and 10c). Also on this plot is a modeled trace assuming a vertical layer 14 cm wide. For the vertical layer, $\varepsilon_r = 4$ and for the water saturated sand beyond the layer, $\varepsilon_r = 24$. Note the anomalous decrease in slope on both traces at approximately 2.5 ns for the physical data and 4 ns for the modeled. Primary differences in the modeled and received waveform are due to multiple reflected arrivals not accounted for in the model. These results suggest that the tool may have detected at least 14 cm into the formation around the borehole.

sand

3%
clay

6%
clay

---

sand

(a) (b)

Figure 18a, b. Photographs of PVC wells after excavation of the tank. The clear PVC east and west wells are shown in Figure 18a. The dielectric tool was logged in the west well at the right in Figure 18a. The PVC seismic wells are shown in Figure 18b; the south receiver well is on the left and the north transmitter well is on the right. The variation in PCE distribution in the layers is evident from the pattern etched and dyed on the surface of the wells from the direct contact with the PCE.

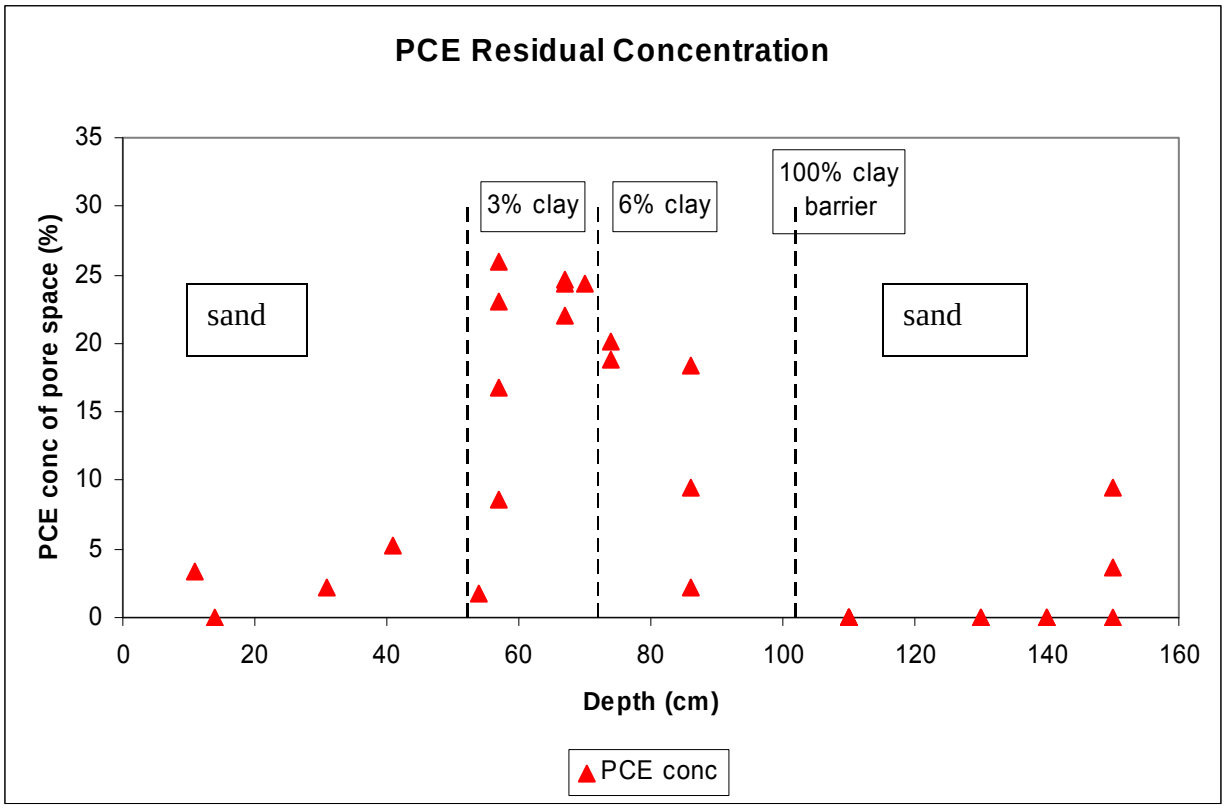

Figure 19. Plot of PCE concentration as a percentage of pore space verses depth. Samples were taken at a number of locations at a particular depth in both the 3% and 6% clay layers and at the bottom of the tank. The range in values at the 55 and 87 cm depths reflect the inhomogeneous distribution of the PCE in the formations. Note these depths are from the surface of the sand; 12 cm should be added for comparison to the dielectric logging measurements (to the top of the west well).

Conclusions

The dielectric logging tool indeed responded to varying degrees of PCE saturations in the tank and successfully monitored PCE movement throughout the experiment. Little attempt was made to interpret the dielectric tool data quantitatively. This is because the tool response in different borehole environments is not completely known at the present time. Interpretation is further complicated by possible asymmetry and inhomogeneity of the PCE saturation around the borehole. Despite these unknowns, numerical simulations that were performed using a simplified model and the FDTD method qualitatively were in agreement with the modeled data. This suggests that relative interpretation of the dielectric tool data is possible. The tool is an excellent anomaly detector and it can determine whether there is a relative increase or decrease in dielectric permittivity in thin zones around the borehole. The modeling also suggests that the tool can detect changes as deep as 14 cm away from the borehole. This is consistent with tests performed by Abraham, 1999a that show the tool having a depth of investigation as far as 25 cm. As a result, the dielectric tool may be helpful in detecting changes of PCE saturation around a borehole during remediation of a contaminated site.

References

Abraham, J.D. 1999a. Physical modeling of a prototype slim-hole time-domain dielectric logging tool. M.Sc. thesis. Colorado School of Mines.

Abraham, J. D., 1999b. "Physical modeling of a prototype slim-hole time-domain dielectric logging tool." In *Proceedings of the Symposium on Application of Geophysics to Engineering and Environmental Problems.* Environmental and Engineering Geophysical Society, 503-512.

Ellefsen, K.J., Abraham, J.D., Wright, D.L. and Mazzella, A.T. 2004. "Numerical study of electromagnetic waves generated by a prototype dielectric logging tool." *Geophysics* (**69**): 64-77.

Greenhouse, J., Brewster, M., Schneider, G., Redman, D., Annan, P., Olhoeft, G., Lucius, J., Sander, K., and Mazzella, A. 1993. "Geophysics and solvents: The Borden experiment." *The Leading Edge* (**12**): 261-267.

Kraus, J.D. 1950. *Antennas*. McGraw-Hill Book Company, Inc., New York.

Lucius, J.E., Olhoeft, G.R., Hill P.L. and Duke, S.K., 1992. *Properties and Hazards of 108 Selected Substances* (1992 ed.). U.S. Geological Survey Open File Report 90-527.

Sears, F.W., Zemansky, M.W., and Young, H.D. 1987. *University Physics.* Addison-Welsley Publishing Company, Reading.

Sheriff, R.E. 1991. *Encyclopedic Dictionary of Exploration Geophysics.* Society of Exploration Geophysics, Tulsa.

Sneddon, K.W., Olhoeft, G.R., Powers, M.H. 2000. "Determining and mapping DNAPL saturation values from noninvasive GPR measurements." In *Proceedings of the Symposium on Application of Geophysics to Engineering and Environmental Problems.* Environmental and Engineering Geophysical Society, 293-302.

Wright, D.L. and Nelson, P.H. 1993. "Borehole dielectric logging: a review and laboratory experiment." In *Proceedings of the 5th Int. Symp. on Geophysics for Minerals, Geotechnical and Environmental Applications.* Minerals and Geotechnical Logging Society, paper T.

Wright, D.L., Abraham, J.D., Ellefsen, K.J., and Rossabi, J. 1998. "Borehole radar tomography and dielectric logging at the Savannah River Site." In *Proceedings of the 7th Inter. Conf. on GPR,* 539-544.

United States
Environmental Protection
Agency

Office of Research
And Development (8101R)
Washington, DC 20460

Official Business
Penalty for Private Use
$300

EPA/600/R-06/092
September 2006
www.epa.gov

Please make all necessary changes on the below label, detach or copy, and return to the address in the upper left-hand corner.

If you do not wish to receive these reports CHECK HERE ☐; detach, or copy this cover, and return to the address in the upper left-hand corner.

PRESORTED STANDARD
POSTAGE & FEES PAID
EPA
PERMIT No. G-35